Available online at www.sciencedirect.com

ScienceDirect

Mendeleev Commun., 2022, **32**, 615–618

Mendeleev Communications

Simultaneous formation of P–C/P–O-cage phosphoranes in the reaction of 2-[(2-methylcarbonyl)phenyloxy]-4,4,5,5-tetramethyl-1,3,2-dioxaphospholane with hexafluoroacetone

Vladimir F. Mironov,* Mudaris N. Dimukhametov, Igor A. Litvinov and Aidar T. Gubaidullin

A. E. Arbuzov Institute of Organic and Physical Chemistry, FRC Kazan Scientific Center of the Russian Academy of Sciences, 420088 Kazan, Russian Federation. E-mail: mironov@iopc.ru

DOI: 10.1016/j.mencom.2022.09.015

Reaction of 2-[(2-methylcarbonyl)phenyloxy]-4,4,5,5-tetramethyl-1,3,2-dioxaphospholane with hexafluoroacetone leads to the simultaneous formation of two P–C/P–O-cage phosphoranes. The P–C-cage species does not convert to the P–O-cage one neither under the kinetically (3 years, 20–25 °C, dichloromethane) nor under the thermodynamically controlled conditions (110 °C, toluene, 8 h).

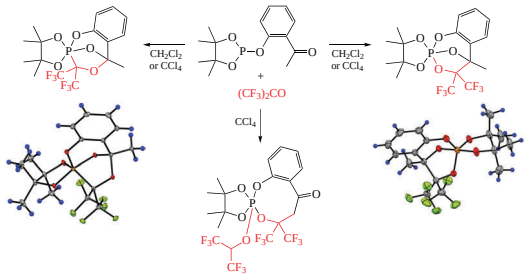

Keywords: 1,3,2-dioxaphospholanes, hexafluoroacetone, aldol reaction, PCO/POC-rearrangement, cage phosphoranes, spirophosphoranes.

Pentacoordinated phosphorus derivatives attract the attention of researchers due to several reasons. They are intermediates in the nucleophilic substitution reactions at tetracoordinated phosphorus,[1] among which the reactions of phosphorylation and dephosphorylation occur in living cells.[2] Phosphoranes are the intermediates in the Mitsunobu reaction,[3] the Kukhtin–Ramiretz reaction,[4] the ligand coupling reaction at pentacoordinated phosphorus,[5] desulfurization with trialkyl phosphites,[6] and in the synthesis of isoquinolines from alkynes, nitriles and triphenylphosphine.[7] Phosphoranes have recently been shown to be intermediates in the unusual carbofluorination of alkynes with acyl fluorides and phosphines,[8] as well as coupling reaction of acyl fluorides, silylenols, and alkynes leading to variously functionalized 1,3-dienes.[9] Much attention is paid both to the development of new methods for the synthesis of phosphoranes[10] and to the study of their structure[11] and chemical properties.[12]

In recent years, we have been developing a new method for the synthesis of cage phosphoranes based on the intramolecular cascade reactions of cyclic P^{III} derivatives containing a carbonyl group in the exocyclic substituent.[13] Cage phosphoranes are convenient models for studying the reactivity of pentacoordinated phosphorus derivatives due to the rigidity of the structure, which limits intramolecular ligand rearrangements at the phosphorus atom. We have shown that P–C-cage phosphoranes can undergo P–CO/P–OC rearrangement which proceeds with a high stereoselectivity through a possible intermediate of the oxaphosphirane type.[14]

In this work, in order to study the boundaries of this rearrangement, we subjected hexafluoroacetone to the reation with special P^{III} derivative, 2-[(2-methylcarbonyl)phenoxy]-4,4,5,5-tetramethyl-1,3,2-dioxaphospholane **1**, containing a carbonyl group in a spatially rigid exocyclic substituent. The reaction of dioxaphospholane **1** with hexafluoroacetone was carried out under two different conditions: (*a*) in dichloromethane and (*b*) in tetrachloromethane as solvents at –40 °C with a two-fold excess of hexafluoroacetone. The process in variant (*a*) gave the mixture of P–C- and P–O-phosphoranes **2**, **3** (Scheme 1) in the ratio 5 : 9 (see also Online Supplementary Materials, Figure S43). These compounds reveal the same molecular ion peak 448 in the electron ionization (EI) mass spectrum, which confirms their isomeric composition consisting of one molecule of phospholane **1** and one molecule of hexafluoroacetone. Both compounds were isolated by fractional crystallization from various solvents. Their structures were determined by ^{1}H, ^{19}F–{^{1}H}, ^{31}P–{^{1}H}, ^{13}C–{^{1}H}, ^{13}C–{^{1}H}–dept, ^{13}C NMR spectroscopy as well as X-ray diffraction study (Figures 1 and 2).†

† *Crystal data for* **2** at 100 K. $C_{17}H_{19}F_6O_5P$ (M = 448.29), monoclinic, space group $P2_1/c$, at 100(2) K, a = 12.8493(7), b = 9.8769(5) and c = 15.0305(9) Å, β = 99.350(2)°, V = 1882.20(18) Å^3, Z = 4, d_{calc} = 1.582 g cm^{-3}, μ(MoKα) = 0.231 mm^{-1}, F(000) = 920. 38897 reflections were measured and 5968 independent reflections (R_{int} = 0.038) were used in a further refinement. The refinement converged to wR_2 = 0.0869 and GOF = 1.03 for all independent reflections [R_1 = 0.0349 was calculated against F for 4971 observed reflections with $I > 2\sigma(I)$].

Crystal data for **2** at 296 K. $C_{17}H_{19}F_6O_5P$ (M = 448.29), monoclinic, space group $P2_1/c$, at 296(2) K, a = 12.972(6), b = 9.919(4) and c = 15.183(7) Å, β = 99.482(6)°, V = 1926.9(15) Å^3, Z = 4, d_{calc} = 1.545 g cm^{-3}, μ(MoKα) = 0.226 mm^{-1}, F(000) = 920. 16448 reflections were measured and 3783 independent reflections (R_{int} = 0.048) were used in a further refinement. The refinement converged to wR_2 = 0.1011 and GOF = 1.024 for all independent reflections [R_1 = 0.0618 was calculated against F for 2797 observed reflections with $I > 2\sigma(I)$].

Crystal data for **3** at 296 K. $C_{17}H_{19}F_6O_5P$ (M = 448.29), monoclinic, space group $P2_1/c$, at 296(2) K, a = 14.320(4), b = 10.422(3) and c = 12.856(4) Å, β = 94.930(4)°, V = 1911.6(10) Å^3, Z = 4, d_{calc} = 1.558 g cm^{-3}, μ(MoKα) = 0.228 mm^{-1}, F(000) = 920. 14497 reflections were measured and 3744 independent reflections (R_{int} = 0.032) were used in a further refinement. The refinement converged

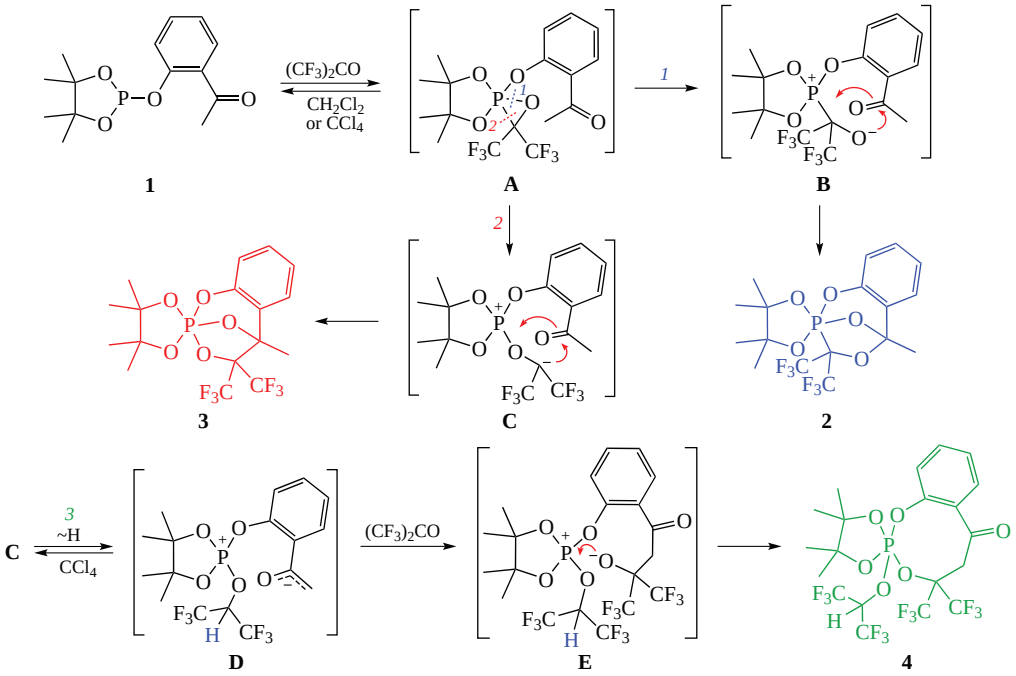

Scheme 1

The process apparently begins with a cheletropic [1+2]-cycloaddition and leads to an intermediate **A**, a three-membered oxaphosphirane with a pentacoordinated phosphorus atom. The subsequent transformations can include both the breakage of the P–O bond (pathway ***1***) and P–C bonds (pathway ***2***) (see Scheme 1). When pathway *1* is realized, cage phosphorane **2** is formed through the P^+–C–O^- bipolar ion intermediate **B**. Process ***2*** leads to a cage pentaalkoxyphosphorane **3** *via* P^+–O–C^- bipolar ion intermediate **C**. Both pathways ***2*** and ***1*** are irreversible, *i.e.* heating of P–C-species **2** in toluene (110 °C, 8 h) does not afford compound **3**, the product of the P^V–C–O → P^V–O–C rearrangement. We have previously found this compound among the P^V–C-products of the reaction between 4,5-dimethyl-2-(2-oxo-1,2-diphenylethoxy)-1,3,2-dioxaphospholane or 4,4,5,5-tetramethyl-2-(2-oxo-1,2-diphenylethoxy)-1,3,2-dioxaphospholane with hexafluoroacetone.[13]

Under these hard conditions, compound **2** would decompose into the starting dioxaphospholane **1** and hexafluoroacetone (see Online Supplementary Materials, Figure S42). This unusual fact was evidenced from ^{31}P–{^1H} NMR spectroscopy study when chemical shift corresponding to the P^{III} derivative (δ_P 139.1 ppm) appeared. Long-term (more than 3 years) storage of P–C-phosphorane **2** under kinetically controlled conditions (dichloromethane solution at 20–25 °C) also did not lead to its isomerization into P–O-species **3**. This indicates the irreversible nature of both the P–O bond cleavage process in intermediate **A** (pathway ***1***) and P–C-phosphorane **2** formation.

The reaction of dioxaphospholane **1** with hexafluoroacetone in tetrachloromethane unexpectedly afforded three derivatives with a pentacoordinated phosphorus atom, namely, cage phosphoranes **2** and **3** (5 : 2) and spirophosphorane **4** in which the phosphorus atom was included in an eight-membered cycle. The EI mass spectrum contains two peaks corresponding to the products' molecular ions of 1:1 reactant composition (448) and that of 1 : 2 (614), the ratio of phosphoranes (**2**+**3**)/**4** having been 14 : 5.

The formation of spirophosphorane **4** occurs along pathway ***3*** (see Scheme 1) which includes the enolization of the methylcarbonyl group in the bipolar ion **C** followed by the proton transfer to the carbanion center of the $(CF_3)_2C^-$ moiety. The more stabilized bipolar ion **D** that is generated would undergo the aldol reaction with the second molecule of hexafluoroacetone to form bipolar ion **E** which is further converted into spirophosphorane **4**. It was not possible to isolate compound **4**, however, its main structural fragments such as hexafluoroisopropyl group, *gem*-trifluoromethyl fragment and methylene group, were identified by ^{19}F–{^1H}, ^1H, ^{31}P–{^1H} and ^{31}P NMR methods. In the ^{31}P–{^1H} NMR spectrum, it corresponds to a singlet (δ_P –64.5 ppm), which turns into a doublet in the ^{31}P NMR spectrum ($^3J_{HCOP}$ 14.6 Hz) (see Figures S6 and S7).

In the ^{19}F–{^1H} NMR spectrum (Figure S8), compound **4** shows two quartets (δ_F –77.69 and –78.50 ppm, $^4J_{FF}$ 10.0 Hz) corresponding to the *gem*-trifluoromethyl fragment (A_3X_3-system), and two multiplets (δ_F –74.03 and –74.14 ppm, $^4J_{FF}$ 8.6 Hz) corresponding to the hexafluoroisopropyl substituent (A_3B_3-system). In the low-field region of ^1H NMR spectrum, a doublet of septets (δ 5.41 ppm, $^3J_{POCH}$ 14.5 Hz, $^3J_{FCCH}$ 5.9 Hz) and two broad singlets (δ 5.40 and 5.94 ppm) appear being typical of the proton in the hexafluoroisopropyl substituent fragment and non-equivalent protons of the methylene group in the CH^AH^X–C(O) fragment.

According to X-ray study (see Figures 1 and 2), the phosphorus atom geometries in both molecules **2** and **3** appear

---

to $wR_2 = 0.0889$ and GOF = 1.03 for all independent reflections [$R_1 = 0.0355$ was calculated against F for 2763 observed reflections with $I > 2\sigma(I)$].

The X-ray diffraction data for the crystals **2** (296 K) and **3**, were collected on a Bruker Smart ApexII CCD diffractometer at room temperature [296(2) K], and for **3** (100 K) were collected on a Bruker Kappa Apex II CCD diffractometer at low temperature [100(2) K], in the ω and φ-scan modes using graphite monochromated MoKα (λ = 0.71073 Å) radiation. Data were corrected for the absorption effect using SADABS program.[15] Data collection: images were indexed and integrated using the APEX2 data reduction package.[16] The structures were solved by direct method using SHELXT[17] and refined by the full matrix least-squares using SHELXL programs[18] in the program package WinGX.[19] Hydrogen atoms in all structures were inserted at calculated positions and refined as riding atoms. Analysis of the intermolecular interactions was performed using the program PLATON.[20] Mercury program package[21] was used for figures preparation.

CCDC 2149603–2149605 contain the supplementary crystallographic data for this paper. These data can be obtained free of charge from the Cambridge Crystallographic Data Centre *via* http://www.ccdc.cam.ac.uk.

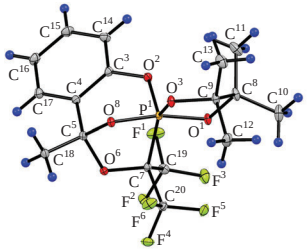

Figure 1 Geometry of molecule **2** in the crystal ($P^1_RC^5_S$/$P^1_SC^5_R$-diastereoisomer, $P^1_RC^5_S$-enantiomer is shown). Non-hydrogen atoms are shown as thermal ellipsoids with a probability of 50%. Hydrogen atoms are shown as spheres of arbitrary radius. Selected bond lengths (Å) and bond angles (deg): P^1–O^1 1.636(1), P^1–O^2 1.6039(8), P^1–O^3 1.6072(9), P^1–O^8 1.6679(9), P^1–C^7 1.936(1), O^1–P^1–O^2 95.73(5), O^1–P^1–O^3 91.75(4), O^1–P^1–O^8 167.12(5), O^1–P^1–C^7 89.10(5), O^2–P^1–O^3 114.43(5), O^2–P^1–O^8 96.89(4), O^2–P^1–C^7 106.75(5), O^3–P^1–O^8 113.81(7), O^8–P^1–C^7 84.80(5).

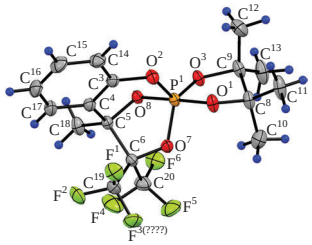

Figure 2 Geometry of molecule **3** in the crystal ($P^1_SC^5_S$/$P^1_RC^5_R$-diastereoisomer, $P^1_SC^5_S$-enantiomer is shown). Non-hydrogen atoms are shown as thermal ellipsoids with a probability of 30%. Hydrogen atoms are shown as spheres of arbitrary radius. Selected bond lengths (Å) and bond angles (deg): P^1–O^1 1.632(2), P^1–O^2 1.611(2), P^1–O^3 1.590(2), P^1–O^7 1.634(2), P^1–O^8 1.669(2), O^1–P^1–O^2 89.57(8), O^1–P^1–O^3 92.06(8), O^1–P^1–O^7 89.64(8), O^1–P^1–O^8 176.30(8), O^2–P^1–O^3 122.98(9), O^2–P^1–O^7 108.90(8), O^2–P^1–O^8 94.07(8), O^3–P^1–O^7 128.10(8), O^3–P^1–O^8 85.39(7), O^7–P^1–O^8 89.82(7).

as slightly distorted trigonal bipyramids. The O^1 and O^8 atoms are in the axial position in both structures; moreover, the O^1–P^1–O^8 bond angles are 176.29(8)° and 167.14(5)°, respectively. Some distortion of the phosphorus configuration in molecule **2** can be explained by the steric reasons, namely, the proximity of trifluoromethyl and methyl substituents to the polycyclic scaffold. The sum of the bond angles at phosphorus in the planar base of the bipyramid of structures **2** and **3** is close to the ideal 359.67(4)° and 358.98(6)°. The P^1–O^8 axial bond length in both molecules is the same within the experimental errors [1.6683(8) and 1.669(2) Å]; the axial P^1–O^4 bond length is somewhat shorter [1.637(1) and 1.632(2) Å]. The equatorial P–O bonds have a shorter length within 1.590(2)–1.634(2) Å, the P^1–C^7 bond length in molecule **2** is 1.936(1) Å. Despite the isomeric differences in the structures of phosphoranes **2** and **3**, the conformation of the bicyclooctane backbone is the same in both molecules (see Online Supplementary Materials, Figure S3). The conformation of the six-membered heterocycle $P^1O^2C^3C^4C^5O^8$ can be described as *sofa*-O^8 (or *envelope*-O^8), the $P^1O^2C^3C^4C^5$ fragment is approximately planar, and the O^8 atom deviates from this plane by the 0.778(3) Å for **2** and 0.841(4) Å for **3**.

According to the PLATON program, the five-membered dioxaphospholane ring $P^1O^8C^5C^6O^7$ of molecule **3** has a *twist* conformation, and the corresponding 1,3,5-dioxaphospholane ring $P^1O^8C^5O^6C^7$ of molecule **2** is defined as an *envelope*-O^8, although the overlap of these fragments is almost complete. The conformation of the seven-membered ring $P^1O^2C^3C^4C^5O^6C^7$ in molecule **2** can be described as a *sofa* with the deviation of the O^6 and C^7 atoms from the remaining planar five-atom fragment by 1.333(3) and 1.529(3) Å, respectively. The 7-membered cycle $P^1O^2C^3C^4C^6O^7$ in the molecule **3** also adopts *sofa* conformation: the $P^1O^2C^3C^4C^5$ fragment is planar; the C^6 and O^6 atoms are deviated from it by 1.279(4) and 1.389(4) Å. The conformation of the spiro-linked dioxaphospholane ring $P^1O^9C^{10}C^{11}O^{12}$ in both molecules is *envelope*-C^{10}, but in molecule **3** the C^{10} atom deviates towards the O^7 atom (closer to the trifluoromethyl substituents), while in the molecule **2** it deviates towards the O^2 atom, opposite to closely spaced trifluoromethyl substituents.

In summary, the reaction outcome of 2-[(2-methylcarbonyl)-phenyloxy]-4,4,5,5-tetramethyl-1,3,2-dioxaphospholane **1** with hexafluoroacetone depends on the nature of the solvent. Cage P–C and P–O phosphoranes **2** and **3** with the ratio of 5:9 are formed in dichloromethane. In tetrachloromethane, along with the formation of compounds **2** and **3**, an aldol reaction occurs with the participation of the methylcarbonyl group of reactant **1** and leads to the spirophosphorane derivative, namely, 2-[(1,1,1,3,3,3-hexafluoropropan-2-yl)oxy]-4′,4′,5′,5′-tetramethyl-4,4-bis(trifluoromethyl)-4,5-dihydro-6*H*-2λ^5-spiro-[benzo[*d*][1,3,2]dioxaphosphocine-2,2′-[1,3,2]dioxaphospholan]-6-one **4**. Under both kinetically and thermodynamically controlled conditions the rearrangement of P–C-cage phosphorane **2** into P–O-cage species **3** does not occur.

Authors thank the staff at the Joint Spectral-Analytical Center for Physicochemical Studies of the Structure, Properties and Composition of Substances and Materials of the Kazan Scientific Center of the Russian Academy of Sciences for technical support of investigations.

Online Supplementary Materials

Supplementary data associated with this article can be found in the online version at doi: 10.1016/j.mencom.2022.09.015.

References

1 (*a*) O. I. Kolodiazhnyi and A. Kolodiazhna, *Tetrahedron: Asymmetry*, 2017, **28**, 1651; (*b*) V. B. Silva, R. B. Campos, P. Pavez, M. Medeiros and E. S. Orth, *Chem. Rec.*, 2021, **21**, 2638; (*c*) J. Lanuza, Á. Sánchez-González, N. A. G. Bandeira, X. Lopez and A. Gil, *Inorg. Chem.*, 2021, **60**, 11177; (*d*) G. I. Kalu, C. I. Ubochi and I. Onyido, *RSC Adv.*, 2021, **11**, 8833; (*e*) M. Mikołajczyk, B. Ziemnicka, J. Krzywański, M. Cypryk and B. Gostyński, *Molecules*, 2021, **26**, 3655; (*f*) M. Mikołajczyk, M. Cypryk, B. Gostyński and J. Kowalczewski, *Molecules*, 2022, **27**, 599.

2 (*a*) R. Micura and C. Höbartner, *Chem. Soc. Rev.*, 2020, **49**, 7331; (*b*) T. J. Wilson and D. M. J. Lilley, in *Ribozymes*, eds. S. Müller, B. Masquida and W. Winkler, Wiley-VCH, 2021, vol. 2, pp. 55–90; (*c*) S. L. Dürr, O. Bohuszewicz, D. Berta, R. Suardiaz, P. G. Jambrina, C. Peter, Y. Shao and E. Rosta, *ACS Catal.*, 2021, **11**, 7915; (*d*) R. Recabarren, K. Zinovjev, I. Tuñón and J. Alzate-Morales, *ACS Catal.*, 2021, **11**, 169; (*e*) K. L. Vay, E. Salibi, E. Y. Song and H. Mutschler, *Chem. – Asian J.*, 2020, **15**, 214.

3 Y. Zou, J. J. Wong and K. N. Houk, *J. Am. Chem. Soc.*, 2020, **142**, 16403.

4 V. F. Mironov, M. N. Dimukhametov, G. A. Ivkova, K. R. Khayarov, D. R. Islamov and I. A. Litvinov, *Chem. Commun.*, 2021, **57**, 8516.

5 (*a*) M. C. Hilton, X. Zhang, B. T. Boyle, J. V. Alegre-Requena, R. S. Paton and A. McNally, *Science*, 2018, **362**, 799; (*b*) X. Zhang, K. G. Nottingham, C. Patel, J. V. Alegre-Requena, J. N. Levy, R. S. Paton and A. McNally, *Nature*, 2021, **594**, 217.

6 A. Gese, M. Akter, G. Schnakenburg, A. G. Alcaraz, A. E. Ferao and R. Streubel, *New J. Chem.*, 2020, **44**, 17122.

7 H. Cui, J. Bai, T. Ai, Y. Zhan, G. Li and H. Rao, *Org. Lett.*, 2021, **23**, 4023.

8 H. Fujimoto, T. Kodama, M. Yamanaka and M. Tobisu, *J. Am. Chem. Soc.*, 2020, **142**, 17323.

9 H. Fujimoto, M. Kusano, T. Kodama and M. Tobisu, *J. Am. Chem. Soc.*, 2021, **143**, 18394.

10 (*a*) H. Fujimoto, M. Kusano, T. Kodama and M. Tobisu, *Org. Lett.*, 2020, **22**, 2293; (*b*) J. Abbenseth and J. M. Goicoechea, *Chem. Sci.*, 2020, **11**, 9728; (*c*) V. O. Smirnov, A. D. Volodin, A. A. Korlyukov and A. D. Dilman, *Chem. Commun.*, 2021, **57**, 4823; (*d*) J. Ponce-de-León, R. Infante and P. Espinet, *Chem. Commun.*, 2021, **57**, 5458; (*e*) H. W. Moon, A. Maity and A. T. Radosevich, *Organometallics*, 2021, **40**, 2785; (*f*) J. G. López, F. L. Ortiz, P. M. S. Peraza, Y. Navarro and M. J. Iglesias, *Synthesis*, 2022, **54**, 600.

11 H. K. Carroll, M. L. Brown, V. C. Yap, J. R. Magnuson, N. A. J. Reich, A. G. P. Macdonald and C. D. Montgomery, *Inorg. Chim. Acta*, 2020, **501**, 119239.
12 (*a*) S. Lim and A. T. Radosevich, *J. Am. Chem. Soc*., 2020, **142**, 16188; (*b*) A. V. Nemtarev, I. O. Nasibullin, R. R. Fayzullin, L. R. Grigor'eva and V. F. Mironov, *Mendeleev Commun*., 2020, **30**, 34; (*c*) W. Ma, W. Dai, Q. Liu, Y. Chen, Y. Zhao and S. Cao, *Tetrahedron*, 2020, **76**, 130886; (*d*) D. Roth, J. Stirn, D. W. Stephan and L. Greb, *J. Am. Chem. Soc*., 2021, **143**, 15845; (*e*) X. Yang, R. Wei, Y. Shi, L. L. Liu, Y. Wu, Y. Zhao and D. W. Stephan, *Chem. Commun*., 2021, **57**, 1194; (*f*) S. A. Föhrenbacher, V. Zeh, M. J. Krahfuss, N. V. Ignat'ev, M. Finze and U. Radius, *Eur. J. Inorg. Chem*., 2021, 1941; (*g*) S. A. Föhrenbacher, M. J. Krahfuss, L. Zapf, A. Friedrich, N. V. Ignat'ev, M. Finze and U. Radius, *Chem. – Eur. J*., 2021, **27**, 3504; (*h*) K. Han, Y. Wang, P. Zhao, X. You, J. Wang, Y. Guo, Y. Zhao and S. Cao, *J. Org. Chem*., 2021, **86**, 4512; (*i*) C.-X. Guo, S. Yogendra, R. M. Gomila, A. Frontera, F. Hennersdorf, J. Steup, K. Schwedtmann and J. J. Weigand, *Inorg. Chem. Front*., 2021, **8**, 2854; (*j*) M. Keßler, B. Neumann, H.-G. Stammler and B. Hoge, *Z. Anorg. Allg. Chem*., 2021, **647**, 225; (*k*) R. Pajkert and G. V. Röschenthaler, in *Organophosphorus Chemistry*, eds. L. J. Higham, D. W. Allen and J. C. Tebby, Royal Society of Chemistry, 2021, vol. 50, pp. 409–428.
13 V. F. Mironov, M. N. Dimukhametov, Ya. S. Blinova and F. Kh. Karataeva, *Russ. J. Gen. Chem*., 2020, **90**, 2080 (*Zh. Obshch. Khim*., 2020, **90**, 1704).
14 (*a*) V. F. Mironov, M. N. Dimukhametov, S. V. Efimov, R. M. Aminova, F. Kh. Karataeva, D. B. Krivolapov, E. V. Mironova and V. V. Klochkov, *J. Org. Chem*., 2016, **81**, 5837; (*b*) N. R. Khasiyatullina, V. F. Mironov, D. B. Krivolapov, E. V. Mironova and O. I. Gnezdilov, *RSC Adv*., 2016, **6**, 85745.
15 G. Sheldrick, *SADABS, Program for Empirical X-ray Absorption Correction*, Bruker-Nonius, 1990–2004.
16 *APEX2 (Version 2.1), SAINTPlus, Data Reduction and Correction Program (Version 7.31A)*, Bruker AXS, Madison, WI, 2006.
17 G. M. Sheldrick, *Acta Crystallogr.*, 2015, **A71**, 3.
18 G. M. Sheldrick, *Acta Crystallogr.*, 2015, **C71**, 3.
19 L. J. Farrugia, *J. Appl. Crystallogr.*, 2012, **45**, 849.
20 A. L. Spek, *Acta Crystallogr.*, 2009, **D65**, 148.
21 C. F. Macrae, P. R. Edgington, P. McCabe, E. Pidcock, G. P. Shields, R. Taylor, M. Towler and J. van de Streek, *J. Appl. Crystallogr*., 2006, **39**, 453.

Received: 11th March 2022; Com. 22/6824